MNRAS **000**, ??–?? (2015) Preprint 16 May 2016 Compiled using MNRAS LATEX style file v3.0

Title

E. Ritondale,[1★] A. N. Other,[2] Third Author[2,3] and Fourth Author[3]
[1]*Max Planck Institute for Astrophysics, Karl-Schwarzschild-Strasse 1, D-85740 Garching, Germany*

Accepted XXX. Received YYY; in original form ZZZ

ABSTRACT
Lyman-alpha emitters (LAEs) are low-mass, high specific star formation rate galaxies that are thought to be predominantly responsible for the reionisation of the Universe. In spite of their importance, it is extremely difficult to characterise in detail all but the brightest, most massive of these galaxies; this is unsatisfactory, since the faint LAE population is expected to contribute significantly to the reionisation. Here we present a study of a new sample of 20 strongly lensed Ly-α emitting galaxies at $z \sim 2.3$, where we take advantage of the lensing magnification (typically a factor of about 20) to characterise some of the physical properties of low star-formation rate LAEs for the first time.

Key words: gravitational lensing – galaxies: structure

1 INTRODUCTION

Lyman-alpha emitting galaxies (LAEs) represent a population of star-forming systems with very large Lyα equivalent widths and some of the highest specific star-formation rates (sSFR) in the Universe, and these low-mass galaxies are thought to be predominantly responsible for the reionisation of the Universe. However, it is extremely difficult to characterise these galaxies in detail because they are intrinsically very faint. Typical LAE galaxies have strong star-formation, high-ionisations, and are typically low metallicity; these properties, combined with a (mostly) low dust content, allow for the escape of a large fraction of Lyα photons. At redshift $2 < z < 3$, well-studied LAEs are typically at the bright end of this parameter space, being L_* galaxies with $M_* \sim 109\ M_\odot$ and typical SFRs of about 30 to 100 $M_\odot$/yr (e.g. Erb et al. 2016), and investigations of lower-SFR objects have generally been limited to quantifying the properties of strong optical lines (e.g. Trainor et al. 2015). For example, Hagen et al. (2016) have recently shown that low-SFR LAEs (M_* as low as $10^7\ M_\odot$ and SFR $\sim$ 1 to 100 $M_\odot$/yr, consistent with local-Universe *green pea* LAEs, e.g., Henry et al. 2015) have optical strong line (H_α and [O iii]) properties consistent with optically-selected star-forming galaxies of the same masses at z $\sim$ 2, but they are unable to directly determine the properties of these galaxies that may affect the UV escape fraction, including the gas metallicity, density, and kinematics, without additional very large investments in telescope time. Strong gravitational lensing can be used to overcome this limitation, but the difficulty is that most strongly lensed galaxies at z $\sim$ 2 are not LAEs, and at present the properties of only three lensed LAEs have been investigated in detail (Christensen et al. 2012; Vanzella et al. 2016). Fortunately, new HST V -band observations of LAE galaxies selected from the BOSS survey have revealed a sample of strongly lensed systems at $\langle z \rangle \sim 2.5$ for which the magnification effect could reveal the detailed structure of these LAEs at scales around 100 pcs. Our subsequent lens modelling shows that the typical lensing magnification of these objects is $\mu \sim 20$ and, after accounting for this magnification, these objects are compact galaxies with SFRs of $\sim$ 12 $M_\odot$/yr (i.e., a factor of 3 to 8 lower than previous detailed studies).

2 OBSERVATIONS

The BLAEs sample was observed with the *Hubble Space Telescope* (*HST*) using the WFC3 camera and the F606W filter between 2015 November and 2016 May (GO: 14189; PI: Bolton). In total, twenty one candidate gravitationally lensed Lyman-alpha emitting galaxies were observed for about 2500 s each. As their redshifts span from $z \sim 2$ to 3, these observations probed the rest-frame ultraviolet emission between 1500 and 2000 Å. The details of the sample and the observations are given in Table **??**.

The data were retrieved from the *HST* archive and processed using the ASTRODRIZZLE task that is part of the DRIZZLEPAC package. Cut-out images for each target are shown in Fig. **??**. Out of the twenty one candidates, three turned out not to be gravitational lenses (SDSS J0054+2944, SDSS J1116+0915 and

★ E-mail: elisa@mpa-graching.mpg.de

© 2015 The Authors

SDSS J1516+4954). SDSS J2245+0040 is not included in our final sample because the uncertain nature of the deflector, which appears to be a spiral galaxy, made identifying the lensed Lyman alpha emission difficult without additional colour information. Therefore, the final BLAEs sample used for our analysis contains seventeen gravitationally lensed Lyman-alpha emitting galaxies.

3 LENS MODELLING

The gravitational lens modelling and source reconstruction of each system was performed using the Bayesian pixelated technique developed by **?**. Briefly, the mass density distribution of the lens is parametrized with an elliptical power-law profile (plus external shear) with a total of eight free parameters,

$$\kappa\left(x,y\right) = \frac{\kappa_0\left(2-\frac{\gamma}{2}\right)q^{\gamma-3/2}}{2\left(q^2\left(x^2+r_c^2\right)+y^2\right)^{(\gamma-1)/2}}\,, \tag{1}$$

where κ is the dimensionless surface mass density (as a function of position x, y), κ_0 is the surface mass density normalization, q is the axial ratio of the elliptical mass distribution, γ is the radial slope of the mass density profile and r_c is the core-radius. In addition, the position angle of the elliptical mass distribution (θ), and the shear strength (Γ) and positional angle (Γ_θ) as also solved for. The dimensionless surface mass density and the Einstein radius ($R_{\rm ein}$) are related to each other via,

$$R_{\rm ein} = \left(\frac{\kappa_0\left(2-\frac{\gamma}{2}\right)q^{(\gamma-2)/2}}{3-\gamma}\right)^{1/(\gamma-1)}\,. \tag{2}$$

The surface brightness distribution of the foreground gravitational lens is simultaneously modelled with the mass distribution and is parametrised using elliptical Sersic profiles

$$I\left(r\right) = I_0\exp\left[\left(-bn\left(\frac{r}{R_e}\right)^{1/n}\right)-1.0\right]\,, \tag{3}$$

where $I(r)$ is the surface brightness at radius r, I_0 is the surface brightness normalization, R_e is the effective radius, n is the Sersic index and b is ??.

The surface brightness distribution of the (lensing corrected) background source is instead reconstructed using a magnification-adaptive Delaunay tessellation and is characterised by a form and level of regularisation, $\mathbf{R_s}$ and λ_s (see **??**, for a more detailed description). This provides a pixellated surface brightness distribution for the reconstructed source that is free from any parameterised assumptions, such as Sersic or Gaussian light profiles, that may not fully account for the clumpy nature of the rest-frame ultraviolet emission from the BLAEs sources.

The modelling procedure is performed in two steps: first we masked out the emission from the lens galaxy and, given the lensed surface brightness distribution $\boldsymbol{d}$, we optimize for the lens mass parameters $\boldsymbol{\eta} = \{\kappa_0, \theta, q, x, y, \gamma, \Gamma, \Gamma_\theta\}$ and the source regularisation level by maximising the posterior probability density,

$$P(\lambda_{\rm s},\boldsymbol{\eta}\,|\,\boldsymbol{d},\mathbf{R}_{\rm s}) = \frac{P(\boldsymbol{d}\,|\,\lambda_{\rm s},\boldsymbol{\eta},\mathbf{R}_{\rm s})P(\lambda_{\rm s},\boldsymbol{\eta})}{P(\boldsymbol{d}\,|\,\mathbf{R}_{\rm s})}\,. \tag{4}$$

At each step of this optimization, the corresponding most probable source $\boldsymbol{s}$ is obtained by maximising the probability density distribution

$$P\left(\boldsymbol{s}\,|\,\boldsymbol{d},\lambda_{\rm s}\boldsymbol{\eta},\mathbf{R}_{\rm s}\right) = \frac{P(\boldsymbol{d}\,|\,\boldsymbol{s},\boldsymbol{\eta})\,P(\boldsymbol{s}\,|\,\lambda_{\rm s},\mathbf{R}_{\rm s})}{P(\boldsymbol{d}\,|\,\lambda_{\rm s},\boldsymbol{\eta},\mathbf{R}_{\rm s})}\,. \tag{5}$$

Then, using this as a starting point, we parametrise the surface brightness distribution of the lens galaxy as a sum of multiple elliptical Sersic profiles, and optimise for the corresponding parameters, $\boldsymbol{\eta}_l = \{....\}$ together with the background source surface brightness distribution. In the third and last step, we optimise simultaneously for the mass and the light distribution of the deflector and the source regularisation level.

4 RESULTS

5 DISCUSSION

REFERENCES

Vegetti S., Koopmans L. V. E., 2009, MNRAS, 392, 945
Vegetti S., Koopmans L. V. E., Auger M. W., Treu T., Bolton A. S., 2014, MNRAS, 442, 2017

Table 1. Add caption here.

Name (SDSS)	z_{lens}	z_{src}	R_{ein}[arcsec]
J0029 + 2544	0.587	2.450	
J0113 + 0250	0.623	2.609	
J0201 + 3228	0.396	2.821	
J0237 − 0641	0.486	2.249	
J0742 + 3341	0.494	2.363	
J0755 + 3445	0.722	2.634	
J0856 + 2010	0.507	2.233	
J0918 + 4518	0.524	2.344	
J0918 + 5104	0.581	2.403	
J1110 + 2808	0.607	2.399	
J1110 + 3649	0.733	2.502	
J1141 + 2216	0.586	2.762	
J1201 + 4743	0.563	2.126	
J1226 + 5457	0.498	2.732	
J1529 + 4015	0.531	2.792	
J2228 + 1205	0.530	2.832	
J2342 − 0120	0.527	2.265	

Table 2. Add caption here. This table should contain the best parameters for the sersic models

Name (SDSS)	n_{Ser}

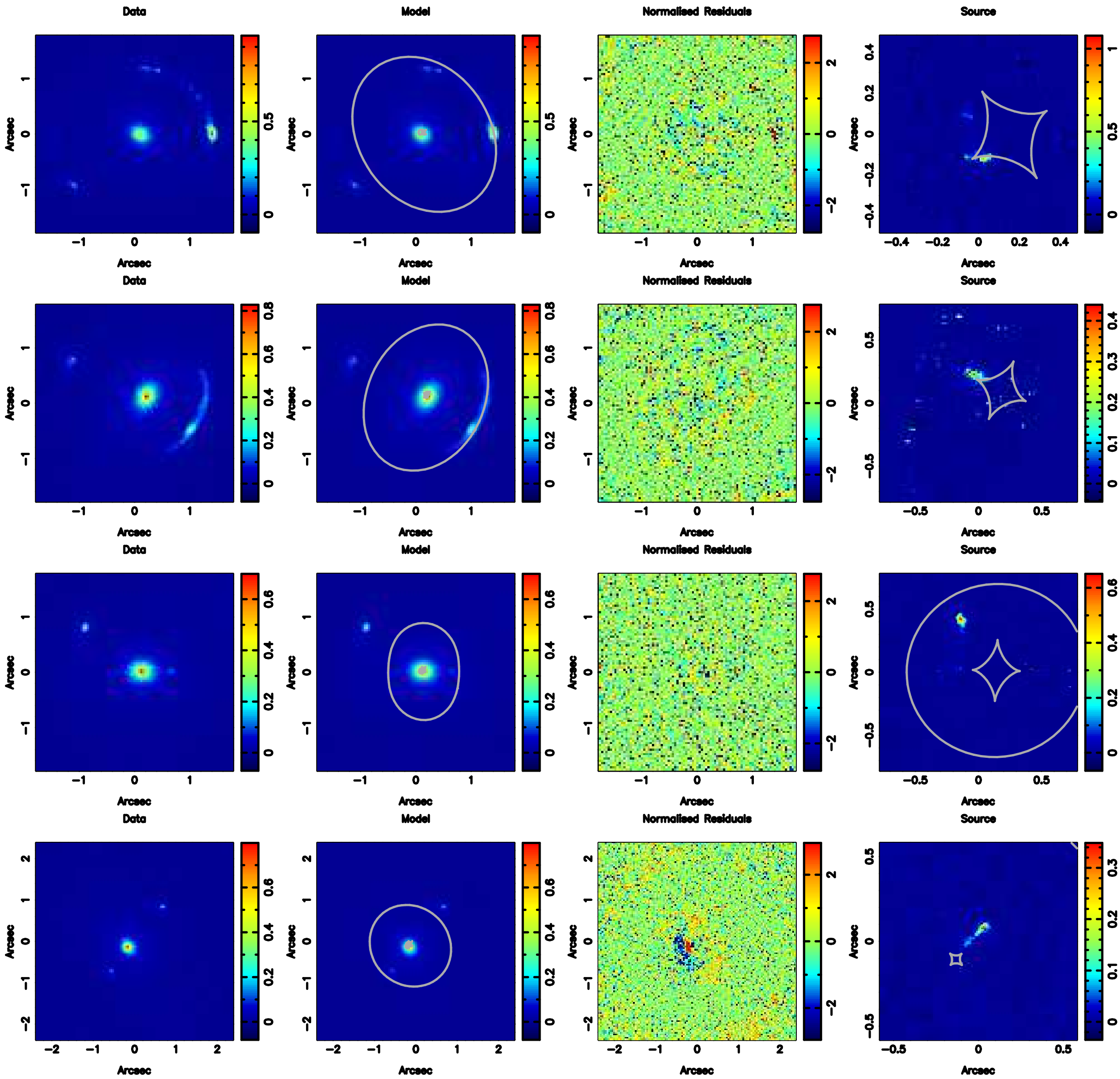

Figure 1. From top to bottom: best models for the lens gravitational systems ..... From left to right: input data, reconstructed model, normalised image residuals and reconstructed source.

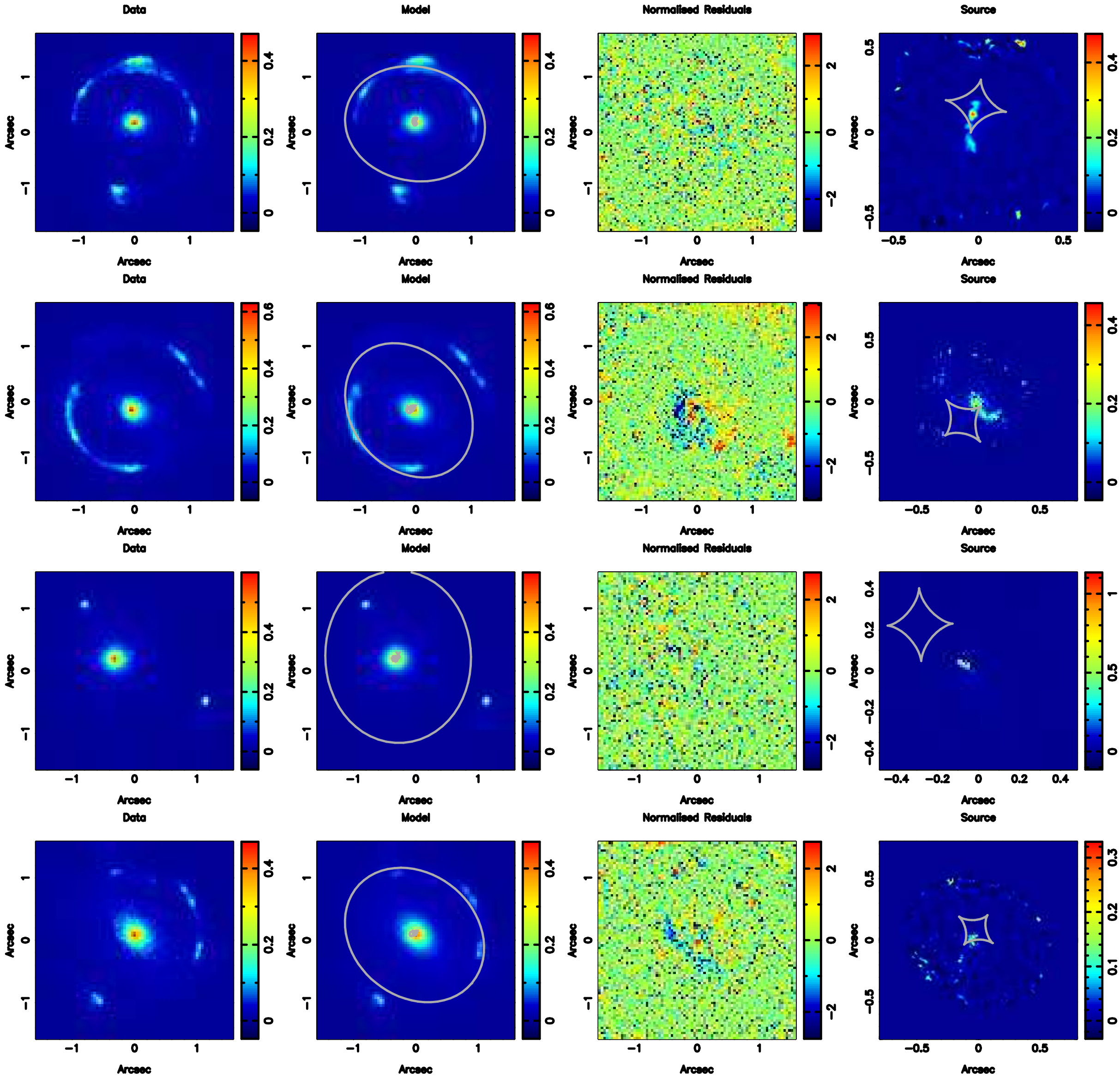

Figure 2. From top to bottom: best models for the lens gravitational systems ..... From left to right: input data, reconstructed model, normalised image residuals and reconstructed source.